ARTICLES

In vitro reprogramming of fibroblasts into a pluripotent ES-cell-like state

Marius Wernig[1]*, Alexander Meissner[1]*, Ruth Foreman[1,2]*, Tobias Brambrink[1]*, Manching Ku[3]*, Konrad Hochedlinger[1]†, Bradley E. Bernstein[3,4,5] & Rudolf Jaenisch[1,2]

Nuclear transplantation can reprogramme a somatic genome back into an embryonic epigenetic state, and the reprogrammed nucleus can create a cloned animal or produce pluripotent embryonic stem cells. One potential use of the nuclear cloning approach is the derivation of 'customized' embryonic stem (ES) cells for patient-specific cell treatment, but technical and ethical considerations impede the therapeutic application of this technology. Reprogramming of fibroblasts to a pluripotent state can be induced *in vitro* through ectopic expression of the four transcription factors Oct4 (also called Oct3/4 or Pou5f1), Sox2, c-Myc and Klf4. Here we show that DNA methylation, gene expression and chromatin state of such induced reprogrammed stem cells are similar to those of ES cells. Notably, the cells—derived from mouse fibroblasts—can form viable chimaeras, can contribute to the germ line and can generate live late-term embryos when injected into tetraploid blastocysts. Our results show that the biological potency and epigenetic state of *in-vitro*-reprogrammed induced pluripotent stem cells are indistinguishable from those of ES cells.

Epigenetic reprogramming of somatic cells into ES cells has attracted much attention because of the potential for customized transplantation therapy, as cellular derivatives of reprogrammed cells will not be rejected by the donor[1,2]. Thus far, somatic cell nuclear transfer and fusion of fibroblasts with ES cells have been shown to promote the epigenetic reprogramming of the donor genome to an embryonic state[3–5]. However, the therapeutic application of either approach has been hindered by technical complications as well as ethical objections[6]. Recently, a major breakthrough was reported whereby expression of the transcription factors Oct4, Sox2, c-Myc and Klf4 was shown to induce fibroblasts to become pluripotent stem cells (designated as induced pluripotent stem (iPS) cells), although with a low efficiency[7]. The iPS cells were isolated by selection for activation of *Fbx15* (also called *Fbxo15*), which is a downstream gene of *Oct4*. This important study left a number of questions unresolved: (1) although iPS cells were pluripotent they were not identical to ES cells (for example, iPS cells injected into blastocysts generated abnormal chimaeric embryos that did not survive to term); (2) gene expression profiling revealed major differences between iPS cells and ES cells; (3) because the four transcription factors were transduced by constitutively expressed retroviral vectors it was unclear why the cells could be induced to differentiate and whether continuous vector expression was required for the maintenance of the pluripotent state; and (4) the epigenetic state of the endogenous pluripotency genes *Oct4* and *Nanog* was incompletely reprogrammed, raising questions about the stability of the pluripotent state.

Here we used activation of the endogenous *Oct4* or *Nanog* genes as a more stringent selection strategy for the isolation of reprogrammed cells. We infected fibroblasts with retroviral vectors transducing the four factors, and selected for the activation of the endogenous *Oct4* or *Nanog* genes. Positive colonies resembled ES cells and assumed an epigenetic state characteristic of ES cells. When injected into blastocysts the reprogrammed cells generated viable chimaeras and contributed to the germ line. Our results establish that somatic cells can be reprogrammed to a pluripotent state that is similar, if not identical, to that of normal ES cells.

Selection of fibroblasts for *Oct4* or *Nanog* activation

Using homologous recombination in ES cells we generated mouse embryonic fibroblasts (MEFs) and tail-tip fibroblasts (TTFs) that carried a neomycin-resistance marker inserted into either the endogenous *Oct4* (Oct4-neo) or *Nanog* locus (Nanog-neo) (Fig. 1a). These cultures were sensitive to G418, indicating that the *Oct4* and *Nanog* loci were, as expected, silenced in somatic cells. These MEFs or TTFs were infected with Oct4-, Sox2-, c-Myc- and Klf4-expressing retroviral vectors and G418 was added to the cultures 3, 6 or 9 days later. The number of drug-resistant colonies increased substantially when analysed at day 20 (Fig. 1i). Most colonies had a flat morphology (Fig. 1h, right) and between 11% and 25% of the colonies were 'ES-like' (Fig. 1h, left) when selection was applied early (Fig. 1k), a percentage that increased at later time points. At day 20, ES-like colonies were picked, dissociated and propagated in G418-containing media. They gave rise to ES-like cell lines (designated as Oct4 iPS or Nanog iPS cells, respectively) that could be propagated without drug selection, displayed homogenous Nanog, SSEA1 and alkaline phosphatase expression (Fig. 1b–g and Supplementary Figs 1 and 5), and formed undifferentiated colonies when seeded at clonal density on gelatin-coated dishes (see inset in Fig. 1b). Four out of five analysed lines had a normal karyotype (Supplementary Table 1).

Although the timing and appearance of colonies were similar between the Oct4 and Nanog selection, we noticed pronounced quantitative differences between the two selection strategies: whereas Oct4-selected MEF cultures had 3- to 10-fold fewer colonies, the fraction of ES-like colonies was 2- to 3-fold higher than in Nanog-selected cultures. Accordingly, approximately four times more Oct4-selected ES-like colonies gave rise to stable and homogenous iPS cell

[1]Whitehead Institute for Biomedical Research and [2]Department of Biology, Massachusetts Institute of Technology, Cambridge, Massachusetts 02142, USA. [3]Molecular Pathology Unit and Center for Cancer Research, Massachusetts General Hospital, Charlestown, Massachusetts 02129, USA. [4]Broad Institute of Harvard and MIT, Cambridge, Massachusetts 02142, USA. [5]Department of Pathology, Harvard Medical School, Boston, Massachusetts 02115, USA. †Present address: Center for Regenerative Medicine and Cancer Center, Massachusetts General Hospital, Harvard Medical School and Harvard Stem Cell Institute, Boston, Massachusetts 02414, USA.
*These authors contributed equally to this work.

lines compared with Nanog-selected ES-like colonies (Fig. 1k). This suggests that although the *Nanog* locus was easier to activate, a higher fraction of the drug-resistant colonies in Oct4-neo cultures was reprogrammed to a pluripotent state. Therefore, the overall estimated efficiency of 0.05–0.1% to establish iPS cell lines from MEFs was similar between Oct4 selection and Nanog selection, despite the larger number of total Nanog-neo resistant colonies (Fig. 1k). Next we investigated the time course of reprogramming by studying the fraction of alkaline-phosphatase-, SSEA1- and Nanog-positive cells in Oct4-selected MEF cultures. Fourteen days after infection some cells had already initiated alkaline phosphatase activity and SSEA1 expression, but lacked detectable amounts of Nanog protein (Fig. 1j), whereas by day 20, alkaline phosphatase and SSEA1 expression had increased and ~8% of the cells were Nanog-positive. Thus, the reprogramming induced by the four transcription factors (Oct4, Sox2, c-Myc and Klf4) is a gradual and slow process.

Expression and DNA methylation

To characterize the reprogrammed cells on a molecular level we used quantitative polymerase chain reaction with reverse transcription (qRT–PCR) to measure the expression of ES-cell- and fibroblast-specific genes. Figure 2a shows that in Oct4 iPS cells the total level of Nanog and Oct4 was similar to that in ES cells but decreased on differentiation to embryoid bodies. MEFs did not express either gene. Using specific primers for endogenous or total *Sox2* transcripts showed that most *Sox2* transcripts originated from the endogenous locus rather than the viral vector (Fig. 2b). In contrast, *Hoxa9* and *Zfpm2* were highly expressed in MEFs but were expressed at very low levels in iPS or ES cells (Fig. 2c). Western blot analysis showed that multiple iPS clones expressed Nanog and Oct4 proteins at similar levels compared to ES cells (Fig. 2d). Finally, we used microarray technology to compare gene expression patterns on a global level. Figure 2f shows that the iPS cells clustered with ES cells in contrast to wild-type or donor MEFs.

To investigate the DNA methylation level of the *Oct4* and *Nanog* promoters we performed bisulphite sequencing and combined bisulphite restriction analysis (COBRA) with DNA isolated from ES cells, iPS cells and MEFs. As shown in Fig. 2g, both loci were demethylated in ES and iPS cells and fully methylated in MEFs. To assess whether the maintenance of genomic imprinting was compromised we

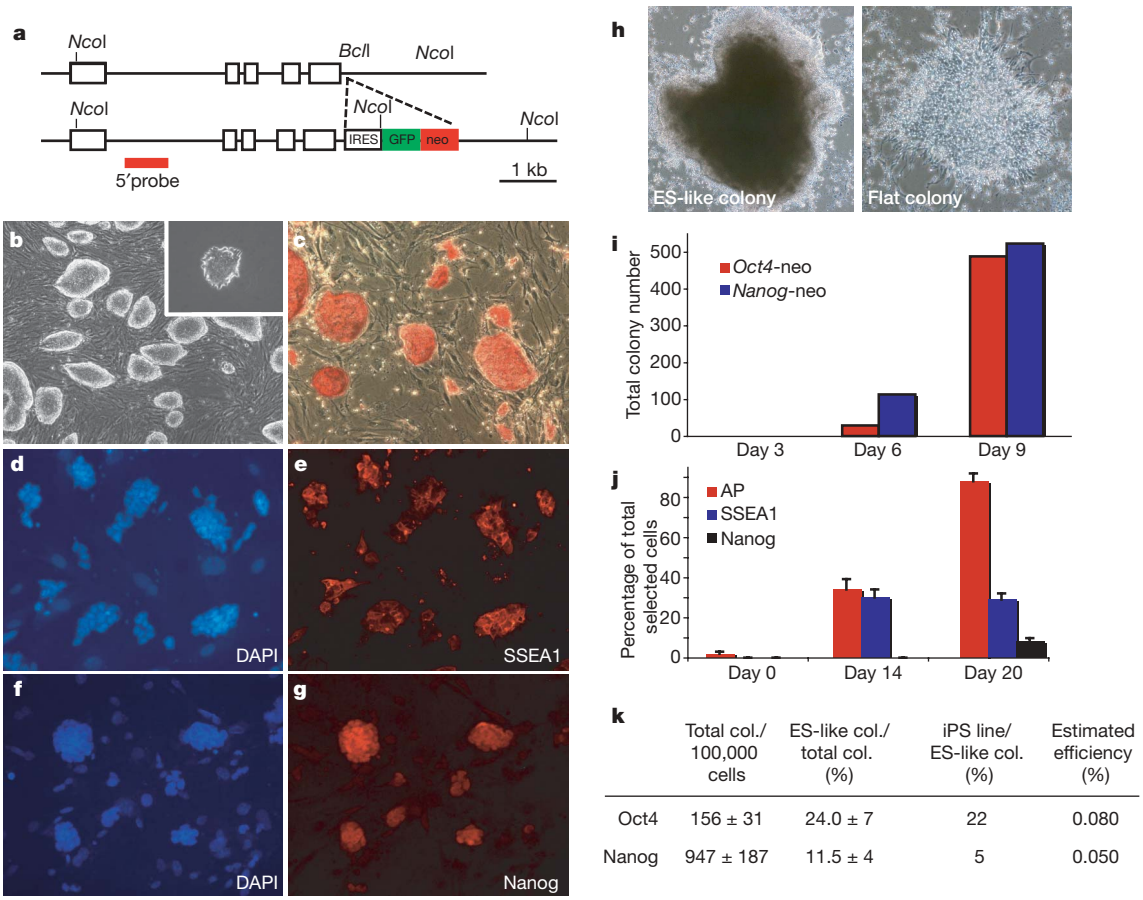

k

	Total col./ 100,000 cells	ES-like col./ total col. (%)	iPS line/ ES-like col. (%)	Estimated efficiency (%)
Oct4	156 ± 31	24.0 ± 7	22	0.080
Nanog	947 ± 187	11.5 ± 4	5	0.050

Figure 1 | Generation of Oct4- and Nanog-selected iPS cells. **a**, Targeting strategy to generate an Oct4-IRES-GFPneo allele. The resulting GFPneo fusion protein has sufficient neomycin-resistance activity in ES cells; GFP fluorescence, however, is not visible. **b**, Phase-contrast micrograph of Oct4 iPS cells (clone 18) grown on irradiated MEFs. Inset: an ES-cell-like colony 5 days after seeding in clonal density without feeder cells. iPS clone 18 cells exhibited strong alkaline phosphatase activity (**c**) and were homogenously labelled with antibodies against SSEA1 (**d**, **e**) and Nanog (**f**, **g**). **h**, One example of an ES-like colony 16 days after infection (left). Most G418-resistant colonies, however, consisted of flat non-ES-like cells (right): **b**, 10×; **c**–**g**, 20×; **h**, 4×. **i**, Gradual activation of the Nanog and Oct4-neo alleles. Shown are the total colony numbers of one experiment at day 20 after infection starting neomycin selection at day 3, 6 and 9. **j**, Fraction of total selected cells expressing alkaline phosphatase, SSEA1 and Nanog 0, 14, and 20 days after infection (counted were more than ten visual fields containing $n > 1{,}000$ total cells for every time point; error bars indicate s.d.). **k**, Estimated reprogramming efficiency of Oct4 selection and Nanog selection ($n = 3$ different experiments; s.e.m. is shown). Indicated are the total number of drug-resistant colonies per 100,000 plated MEFs 20 days after infection; the fraction of ES-like colonies per total number of colonies; the fraction of iPS cell lines that could be established from picked ES-like colonies as defined by homogenous alkaline phosphatase, SSEA1 and Nanog expression. After determining the fraction of *Sox2*- (83.4%), *Oct4*- (53.2%) and *c-myc*- (46.3%) infected MEFs 2 days after infection by immunofluorescence and assuming 50% were infected by *Klf4* viruses, we estimated the overall reprogramming efficiency as the ratio of quadruple-infected cells and the extrapolated total number of iPS cell lines that could be established with G418 selection starting at day 6 after infection.

assessed the methylation status of the four imprinted genes *H19*, *Peg1* (also called *Mest*), *Peg3* and *Snrpn*. As shown in Fig. 2e, bands corresponding to an unmethylated and methylated allele were detected for each gene in MEFs, iPS cells and TTFs. In contrast, embryonic germ cells, which have erased all imprints[8], were unmethylated. Our results indicate that the epigenetic state of the *Oct4* and *Nanog* genes was reprogrammed from a transcriptionally repressed (somatic) to an active (embryonic) state and that the pattern of somatic imprinting was maintained in iPS cells. Furthermore, the presence of imprints suggests a non-embryonic-germ-cell origin of iPS cells.

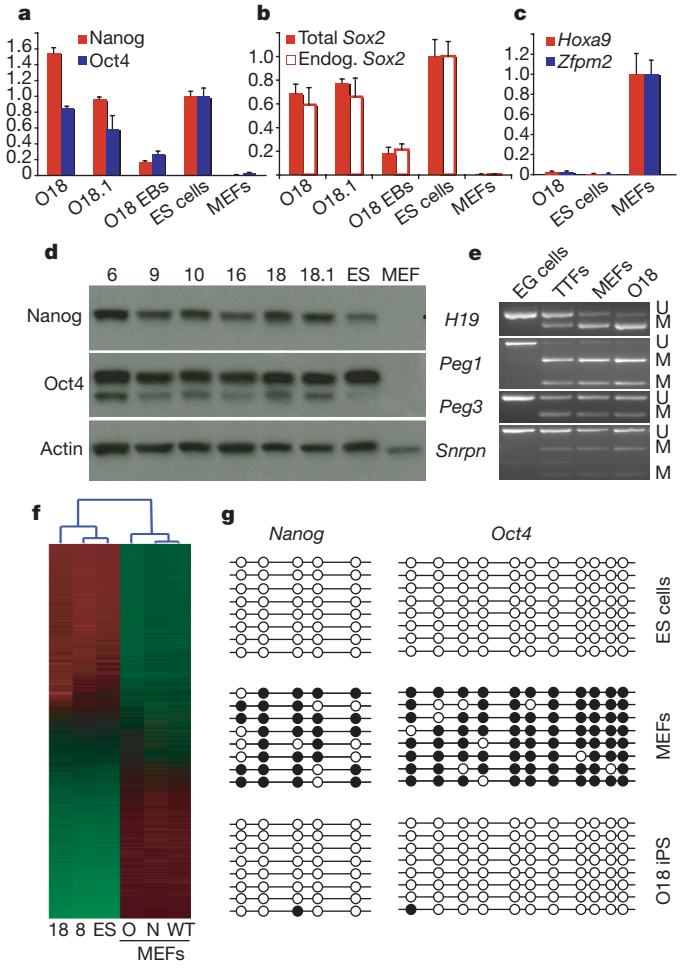

Figure 2 | Expression and promoter methylation analysis of iPS cells. **a**–**c**, qRT–PCR analysis ($n = 3$ independent PCR reactions; error bars indicate s.d.) of Oct4 iPS clone 18, subclone 18.1, 2-week-old embryoid bodies (EBs) derived from clone 18, V6.5 ES cells and Oct4-neo MEFs shows similar Nanog (red bars) and total Oct4 (blue bars) levels as in ES cells (**a**); slightly lower total Sox2 levels (filled red bars), mostly due to expression of endogenous Sox2 transcripts (open red bars, **b**); and strong downregulation of Hoxa9 (red) and Zfpm2 (blue) transcripts in iPS cells (**c**). Transcript levels were normalized to Gapdh expression, with expression levels in ES cells (**a**, **b**) and MEFs (**c**) set as 1. **d**, Western blot analysis for Oct4 and Nanog expression of different Oct4 iPS clones (6, 9, 10, 16, 18) and a GFP-labelled subclone of clone 18 (18.1). **e**, COBRA methylation analysis[32] of imprinted genes *H19* (maternally expressed), *Peg1* (paternally expressed), *Peg3* (paternally expressed) and *Snrpn* (paternally expressed). Upper band, unmethylated (U); lower band, methylated (M). **f**, Unsupervised hierarchical clustering of averaged global transcriptional profiles obtained from Oct4-neo iPS clone 18, Nanog-neo iPS clone 8, genetically matched ES cells (V6.5;129SvJae/C57Bl/6), Oct4-neo MEFs (O), Nanog-neo MEFs (N) and wild-type 129/B6 F1 MEFs (WT). **g**, Analysis of the methylation state of the *Oct4* and *Nanog* promoters using bisulphite sequencing. Open circles indicate unmethylated and filled circles methylated CpG dinucleotides. Shown are eight representative sequenced clones from ES cells (V6.5), Oct4-neo MEFs and Oct4-neo iPS clone 18.

Chromatin modifications

Recently, downstream target genes of *Oct4*, *Nanog* and *Sox2* have been defined in ES cells by genome-wide location analyses[9,10]. These targets include many important developmental regulators, a proportion of which is also bound and repressed by PcG (Polycomb-Group) complexes[11,12]. Notably, the chromatin at many of these non-expressed target genes adopts a bivalent conformation in ES cells, carrying both the 'active' histone H3 lysine 4 (H3K4) methylation mark and the 'repressive' histone H3 lysine 27 (H3K27) methylation mark[13,14]. In differentiated cells, those genes tend instead to carry either H3K4 or H3K27 methylation depending on their expression state. We used chromatin immunoprecipitation (ChIP) and real-time PCR to quantify H3K4 and H3K27 methylation for a set of

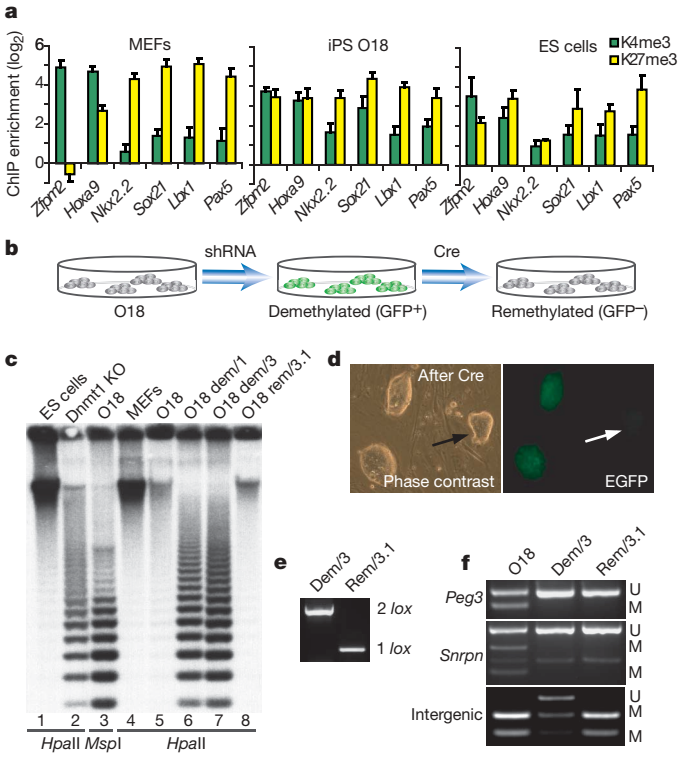

Figure 3 | Reprogrammed MEFs acquire an ES-cell-like epigenetic state. **a**, Real-time PCR after chromatin immunoprecipitation using antibodies against tri-methylated histone H3K4 and H3K27. Shown are the $\log_2$ enrichments for several previously reported 'bivalent' loci in ES cells ($n = 3$ experiments; error bars indicate s.d.). *Zfpm2* and *Hoxa9* show enrichment for the active (H3K4) mark in MEFs and are expressed (Fig. 1c and microarray data), whereas the other tested genes remain silent (microarray data). All loci tested in iPS clone O18 show enrichment for both H3K4 and H3K27 tri-methylation ('bivalent'), as seen in ES cells (V6.5). (See Supplementary Fig. 2 for H3K4 and H3K27 tri-methylation analysis of a subclone (clone O18.1) and Nanog-neo iPS clone N8.) **b**, Experimental design to de- and remethylate genomic DNA. Clone O18 was infected with the *Dnmt1*-hairpin-containing lentiviral vector pSicoR-GFP. The shRNA and GFP marker in the pSicoR vector are flanked by *loxP* sites[18]. Green colonies were expanded and passaged four times. Tat-Cre protein transduction was used to remove the shRNA[33]. **c**, Southern blot analysis of the minor satellite repeats using a methylation-sensitive restriction enzyme (*Hpa*II) and its methyl-insensitive isoschizomer (*Msp*I) as a control. Loss of methylation in two different clones (lanes 6 and 7) is comparable to Dnmt1 knockout ES cells (lane 2). After Cre-mediated recombination, complete remethylation (lane 8) of the repeats is observed within four passages. **d**, **e**, Successful loop out after Tat-Cre treatment was identified by disappearance of EGFP fluorescence (arrow) and verified by PCR analysis (**e**). **f**, COBRA assay of the imprinted genes *Peg3* and *Snrpn* and a random intergenic region close to the *Otx2* locus (Intergenic), demonstrating the expected resistance to *de novo* methylation of imprinted genes in contrast to non-imprinted intergenic sequences. U, unmethylated band; M, methylated band.

genes reported to be bivalent in pluripotent ES cells[13]. Figure 3a shows that the fibroblast-specific genes *Zfpm2* and *Hoxa9* carried stronger H3K4 methylation than H3K27 methylation in the donor MEFs, whereas the silent genes *Nkx2.2*, *Sox1*, *Lbx1* and *Pax5* primarily carried H3K27 methylation. In contrast, in the Oct4 iPS cells, all of these genes showed comparable enrichment for both histone modifications, similar to normal ES cells (Fig. 3a). Identical results were obtained in Nanog iPS clones selected from Nanog-neo MEFs (Supplementary Fig. 2). These data suggest that the chromatin configuration of somatic cells is re-set to one that is characteristic of ES cells.

iPS cells tolerate genomic demethylation

Tolerance of genomic demethylation is a unique property of ES cells in contrast to somatic cells, which undergo rapid apoptosis on loss of the DNA methyltransferase Dnmt1 (refs 15–17). We investigated whether iPS cells would be resistant to global demethylation after Dnmt1 inhibition and would be able to re-establish global methylation patterns after restoration of Dnmt1 activity. To this end, we used a conditional lentiviral vector harbouring a *Dnmt1*-targeting short hairpin (sh)RNA and a green fluorescence protein (GFP) reporter gene (Fig. 3b and ref. 18). Infected iPS cells were plated at low density and GFP-positive colonies were picked and expanded. Southern blot analysis using *Hpa*II-digested genomic DNA showed that global demethylation of infected iPS cells (Fig. 3c, lanes 6, 7) was similar to *Dnmt1*$^{-/-}$ ES cells (lane 2). In contrast, uninfected iPS cells or MEFs (lanes 4, 5) displayed normal methylation levels. Morphologically, the GFP-positive cells were indistinguishable from the parental line or from uninfected sister subclones, indicating that iPS cells tolerate global DNA demethylation. In a second step, the *Dnmt1* shRNA was excised through Cre-mediated recombination and GFP-negative clones were picked (Fig. 3d). The cells had excised the shRNA vector (Fig. 3e) and normal DNA methylation levels were restored (Fig. 3c, lane 8) and were able to generate chimaeras (see below, Table 1), as has been reported previously for ES cells[19]. These observations imply that the *de novo* methyltransferases Dnmt3a and Dnmt3b were reactivated in iPS cells[20], leading to restoration of global methylation levels. As expected[19], the imprinted genes *Snrpn* and *Peg3* were unmethylated and resistant to remethylation (Fig. 3f).

Maintenance of the pluripotent state

Southern blot analysis indicated that Oct4-neo iPS clone 18 carried four to six copies of the *Oct4*, c-*myc* and *Klf4* retroviral vectors and only one copy of the *Sox2* retroviral vector (Fig. 4a). Because these four factors were under the control of the constitutively expressed retroviral long terminal repeat, it was unclear in a previous study why iPS cells could be induced to differentiate[7]. To address this question, we designed primers specific for the four viral-encoded transcription factor transcripts and compared expression levels by qRT–PCR in MEFs 2 days after infection in iPS cells, in embryoid bodies derived from iPS cells, and in demethylated and remethylated iPS cells (Fig. 4b). Although the MEFs represented a heterogeneous population composed of uninfected and infected cells, virally encoded RNA levels of *Oct4*, *Sox2* and *Klf4* RNA were 5-fold higher and of *c-myc* more than 10-fold higher than in iPS cells. This suggests silencing of the viral long terminal repeat by *de novo* methylation during the reprogramming process. Accordingly, the total *Sox2* and *Oct4* RNA levels in iPS cells were similar to those in wild-type ES cells, and the *Sox2* transcripts in iPS cells were mostly, if not exclusively, transcribed from the endogenous gene (compare Fig. 2b). On differentiation to embryoid bodies, both viral and endogenous transcripts were downregulated. All viral *Sox2*, *Oct4* and *Klf4* transcripts were upregulated by approximately twofold in Dnmt1 knockdown iPS cells, and again downregulated on restoration of Dnmt1 activity. This is consistent with previous data that Moloney virus is efficiently *de novo* methylated and silenced in embryonic but not in somatic cells[21,22]. Transcript levels of *c-myc* were about 20-fold lower in iPS cells than in infected MEFs, and did not change on differentiation or demethylation.

To follow the kinetics of vector inactivation during the reprogramming process, we isolated RNA from drug-resistant cell populations at different times after infection. Figure 4c shows that the viral-vector-encoded transcripts were gradually silenced during the transition from MEFs to iPS cells with a time course that corresponded to the gradual appearance of pluripotency markers (compare Fig. 1j). Finally, to visualize directly Oct4 and Nanog expression during differentiation, we injected Oct4 iPS cells into SCID mice to induce teratoma formation (Fig. 4d). Immunostaining revealed that Oct4 and Nanog were expressed in the centrally located undifferentiated cells but were silenced in the differentiated parts of the teratoma (Fig. 4e, f). Our results suggest that the retroviral vectors are subject to gradual silencing by *de novo* methylation during the reprogramming process. The maintenance of the pluripotent state and induction of differentiation strictly depends on the expression and normal regulation of the endogenous *Oct4* and *Nanog* genes.

Developmental potency

We determined the developmental potential of iPS cells by teratoma and chimaera formation. Histological and immunohistochemical analysis of Oct4- or Nanog-iPS-cell-induced teratomas revealed that the cells had differentiated into cell types representing all three embryonic germ layers (Supplementary Figs 3 and 4). To assess more stringently their developmental potential, various iPS cell lines were injected into diploid (2N) or tetraploid (4N) blastocysts. After injection into 2N blastocysts both Nanog iPS and Oct4 iPS clones derived from MEFs (Fig. 5a) or from TTFs (Fig. 5b,c), as well as iPS cells that had been subjected to a consecutive cycle of demethylation and remethylation (compare Fig. 3b, c), efficiently generated viable

Table 1 | Summary of blastocyst infections

Cell line	2N injections				4N injections		
	Injected blastocysts	Live chimaeras	Chimaerism (%)	Germ line	Injected blastocysts	Dead embryos (arrested)	Live embryos (analysed)
O6	ND	ND	ND	ND	13	0	2 (E12.5)
O9	30	5	30–70	Yes	90	3 (E11–13.5)	12 (E10–12.5)
O16	15	3	10–30	Yes	ND	ND	ND
O18	95	8	5–50	No	134	7 (E9–11.5)	4* (E10–12.5)
O3-2	ND	ND	ND	ND	25	2 (E8,11.5)	0
O4-16	ND	ND	ND	ND	35	4 (E11–13.5)	3 (E14.5)
N7	30	1	30	ND	ND	ND	ND
N8	90	14	5–50	No	118	9 (E9–11.5)	1* (E12.5)
N14	30	5	5–20	ND	46	2 (E8,11.5)	1 (E12.5)
TT-O25	50	2	30†	ND	39	3 (E9.5)	0
O18 rem/3.1	25	1	30	ND	ND	ND	ND

The extent of chimaerism was estimated on the basis of coat colour or EGFP expression. ND, not determined. 4N injected blastocysts were analysed between embryonic day E10.5 and E14.5. 'Analysed' indicates the day of embryonic development analysed; 'arrested' indicates the estimated stage of development of dead embryos.
* Developmentally retarded or abnormal. O18 rem/3.1 is a de- and remethylated iPS clone (Fig. 3c).
† On the basis of GFP fluorescence.

high-contribution chimaeras (summarized in Table 1). To test for germline transmission, chimaeras derived from two different iPS lines (Oct4 iPS O9 and O16) were mated with normal females, and blastocysts were isolated and genotyped by three different PCR reactions for the presence of the multiple viral *Oct4* and *c-myc* genes and for the single-copy GFPneo sequences inserted into the *Oct4* locus of the donor cell (Fig. 1a). Figure 5f shows that 9 out of 16 embryos from two chimaeras were positive for the viral copies. As expected, only half of the viral-positive blastocysts contained the GFPneo sequences (5 out of 9 embryos, Fig. 5f, left panel). When embryonic day (E)10 embryos derived from an Oct4 iPS line O16 chimaera were genotyped, three out of eight tested embryos were transgenic (Fig. 5f, right panel). Finally, we injected iPS cells into 4N blastocysts as this represents the most rigorous test for developmental potency, because the resulting embryos are composed only of the injected donor cells ('all ES embryo'). Figure 5d, e shows that both Oct4 and Nanog iPS cells could generate mid- and late-gestation 'all iPS embryos' (summarized in Table 1). These findings indicate that iPS cells can establish all lineages of the embryo and thus have a similar developmental potential as ES cells.

Discussion

The results presented here demonstrate that the four transcription factors Oct4, Sox2, c-myc and Klf4 can induce epigenetic reprogramming of a somatic genome to an embryonic pluripotent state. In contrast to selection for Fbx15 activation[7], fibroblasts that had reactivated the endogenous *Oct4* (Oct4-neo) or *Nanog* (Nanog-neo) loci grew independently of feeder cells, expressed normal Oct4, Nanog and Sox2 RNA and protein levels, were epigenetically identical to ES cells by a number of criteria, and were able to generate viable chimaeras, contribute to the germ line and generate viable late-gestation embryos after injection into tetraploid blastocysts. Transduction of the four factors generated significantly more drug-resistant cells from Nanog-neo than from Oct4-neo fibroblasts but a higher fraction of Oct4-selected cells had all the characteristics of pluripotent ES cells, suggesting that *Nanog* activation is a less stringent criterion for pluripotency than *Oct4* activation.

Our data suggest that the pluripotent state of Oct4 iPS and Nanog iPS cells is induced by the virally transduced factors but is largely maintained by the activity of the endogenous pluripotency factors including Oct4, Nanog and Sox2, because the viral-controlled transcripts, although expressed highly in MEFs, become mostly silenced in iPS cells. The total levels of Oct4, Nanog and Sox2 were similar in iPS and wild-type ES cells. Consistent with the conclusion that the pluripotent state is maintained by the endogenous pluripotency genes is the finding that the *Oct4* and the *Nanog* genes became hypomethylated in iPS cells as in ES cells, and that the bivalent histone modifications of developmental regulators were re-established. Furthermore, iPS cells were resistant to global demethylation induced by inactivation of Dnmt1, similar to ES cells but in contrast to somatic cells. Re-expression of Dnmt1 in the hypomethylated ES cells resulted in global remethylation, indicating that the iPS cells had also reactivated the *de novo* methyltransferases Dnmt3a and Dnmt3b. All these observations are consistent with the conclusion that the iPS cells have gained an epigenetic state that is similar to that of normal ES cells. This conclusion is further supported by the recent observation that female iPS cells, similar to ES cells, reactivate the somatically silenced X chromosome[23].

Expression of the four transcription factors proved to be a robust method to induce reprogramming of somatic cells to a pluripotent state. However, the use of retrovirus-transduced oncogenes represents a serious barrier to the eventual use of reprogrammed cells for therapeutic application. Much work is needed to understand the molecular pathways of reprogramming and to eventually find small

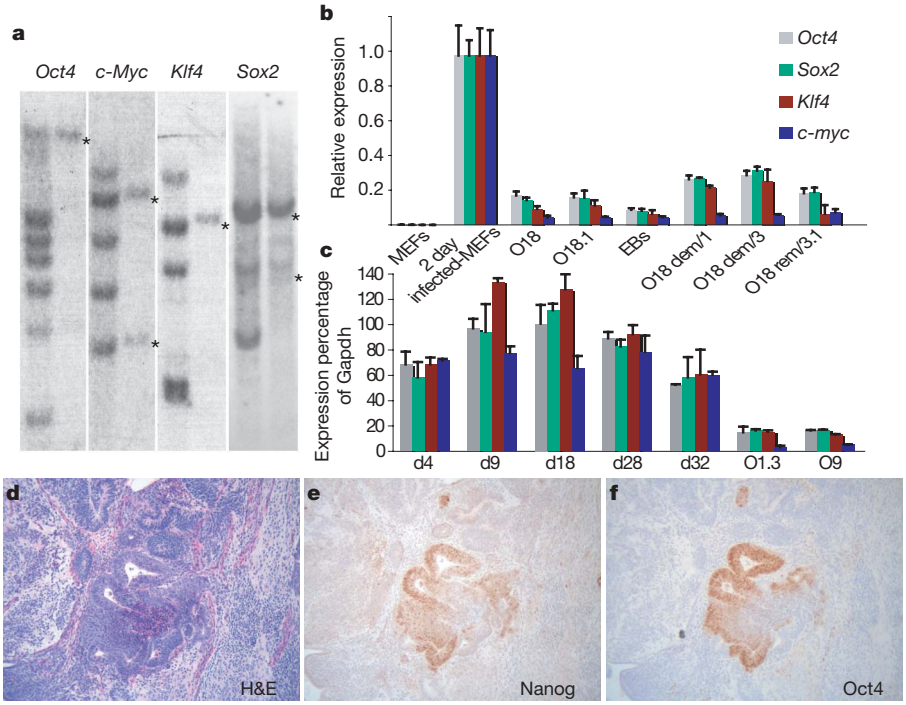

Figure 4 | Efficient silencing of retroviral transcripts in induced pluripotent cells. a, Southern blot analysis of proviral integrations in iPS clone O18 (left lanes) for the four retroviral vectors. Uninfected ES cells (right lanes) show only one or two bands corresponding to the endogenous gene (marked by an asterisk). **b**, Quantitative RT–PCR using primers specifically detecting the four viral transcripts. Shown are Oct4-neo iPS clone 18 and a GFP-labelled subclone, Oct4-neo MEFs, 2-week-old embryoid bodies generated from clone 18, two demethylated clones (18 dem/1 and 18 dem/3), a remethylated clone (18 rem/3.1), and Oct4-neo MEFs 2 days after infection with all four viruses but not selected with G418 ($n = 3$ independent experiments; error bars indicate s.d.). **c**, Viral transcript levels at various time points in cell populations after infection and Oct4 selection and in the two Oct4 iPS cell lines O1.3 and O9 ($n = 3$ independent experiments; error bars indicate s.d.). **d–f**, Paraffin sections of a teratoma 26 days after subcutaneous injection of Oct4 iPS clone 18 cells into SCID mice. H&E, haematoxylin and eosin. Nanog (**e**) and Oct4 (**f**) expression was confined to undifferentiated cell types as indicated an immunohistochemical analysis.

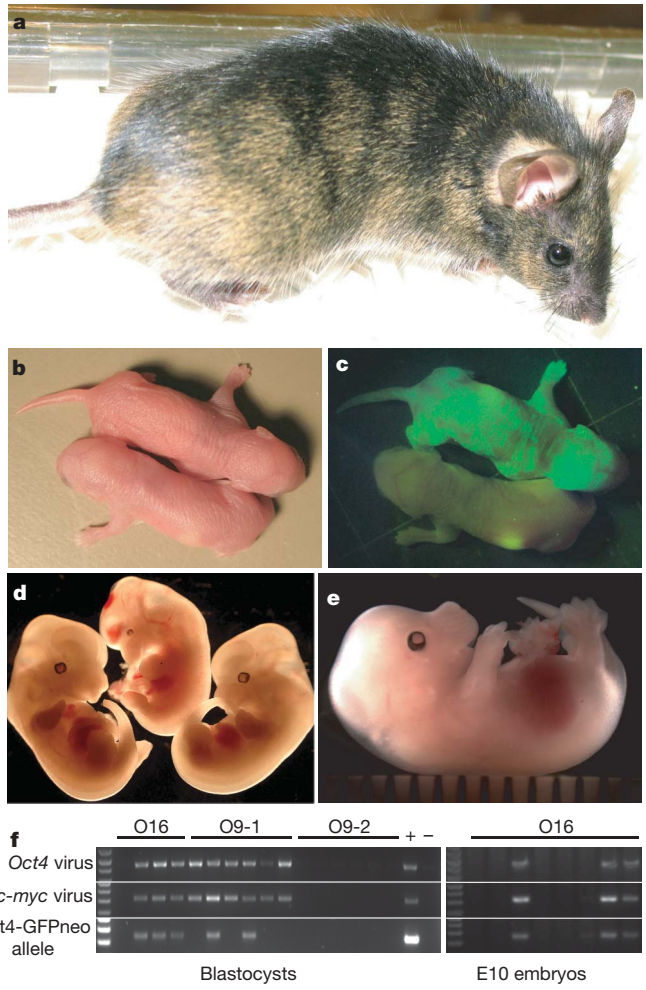

Figure 5 | Developmental pluripotency of reprogrammed fibroblasts. a, A 6-week-old chimaeric mouse. Agouti-coloured hairs originated from Oct4 iPS cell line O18.1. **b**, **c**, Two live pups after 2N blastocyst injection, one of which shows a high contribution (**c**) of the TTF-derived Oct4 iPS cell line TT-O25, which had been GFP-labelled with a lentiviral ubiquitin-EGFP vector. **d**, 'All iPS cell embryos' were generated by injection of iPS cells into 4N blastocysts[34]. Live E12.5 embryos generated from Oct4 iPS line O6 (left), from Nanog iPS line N14 (middle) and from V.6.5 ES cells (right) are shown. **e**, A normally developed E14.5 embryo was derived from Oct4 iPS cell line O4-16 after tetraploid complementation and was isolated by screening MEFs for activation of GFP inserted into the *Oct4* locus. **f**, Germline contribution of Oct4 iPS clones O9 and O16. Genotyping of blastocysts from females mated with three chimaeric males demonstrated the presence of *Oct4* and *c-myc* virus integrations and the Oct4-IRES-GFPneo allele (left panel). Because of the multiple integrations (Fig. 4a) all embryos with iPS cell contribution are expected to be positive for proviral sequences in this assay. In contrast, the single-copy Oct4-IRES-GFPneo allele segregated into only 5 of the 9 virus-positive embryos. All six blastocysts from O9 chimaera 1 were iPS-cell-derived, suggesting that this chimaera was a pseudo-male. Additional genotyping identified 13 out of 72 tested blastocysts derived from iPS line O9 and 4 out of 13 blastocysts derived from iPS line O16 chimaeras carrying the viral transgenes. The right panel shows that 3 out of 8 tested E.10 mid-gestation embryos were sired by a chimaera derived from the donor iPS line O16. +, positive control; −, negative control.

molecules that could achieve reprogramming without gene transfer of potentially harmful genes.

METHODS SUMMARY

Cell culture, gene targeting and viral infections. ES and iPS cells were cultivated on irradiated MEFs. Using homologous recombination we generated ES cells carrying an IRES-GFPneo fusion cassette downstream of *Oct4* exon 5 (Fig. 1a). The *Nanog* gene was targeted as described[24]. Transgenic MEFs were isolated and selected from E13.5 chimaeric embryos after blastocyst injection of Oct4-IRES-GFPneo- or Nanog-neo-targeted ES cells. MEFs were infected overnight with the Moloney-based retroviral vector pLIB (Clontech) containing the murine complementary DNAs of *Oct4*, *Sox2*, *Klf4* and *c-myc*.

Southern blot, methylation and chromatin analyses. To assess the levels of DNA methylation, genomic DNA was digested with *Hpa*II and hybridized to a probe for the minor satellite repeats[25] or with an IAP probe[26]. Bisulphite treatment was performed with the Qiagen EpiTect Kit. For the methylation status of *Oct4* and *Nanog* promoters, bisulphite sequencing analysis was performed as described previously[27]. For imprinted genes, a COBRA assay was performed. PCR primers and conditions were as described previously[28]. The status of bivalent domains was determined by chromatin immunoprecipitation followed by quantitative PCR analysis, as described previously[12]

Expression analysis. Total RNA was reverse-transcribed and quantified using the QuantTtect SYBR green RT–PCR Kit (Qiagen) on a 7000 ABI detection system. Western blot and immunofluorescence analysis was performed as described[29,30]. Microarray targets from 2 μg total RNA were synthesized and labelled using the Low RNA Input Linear Amp Kit (Agilent), hybridized to Agilent whole-mouse genome oligonucleotide arrays (G4122F) and analysed as previously described[31].

Full Methods and any associated references are available in the online version of the paper at www.nature.com/nature.

Received 27 February; accepted 22 May 2007.
Published online 6 June 2007.

1. Hochedlinger, K. & Jaenisch, R. Nuclear transplantation, embryonic stem cells, and the potential for cell therapy. *N. Engl. J. Med.* **349,** 275–286 (2003).
2. Yang, X. *et al.* Nuclear reprogramming of cloned embryos and its implications for therapeutic cloning. *Nature Genet.* **39,** 295–302 (2007).
3. Hochedlinger, K. & Jaenisch, R. Nuclear reprogramming and pluripotency. *Nature* **441,** 1061–1067 (2006).
4. Tada, M., Takahama, Y., Abe, K., Nakatsuji, N. & Tada, T. Nuclear reprogramming of somatic cells by *in vitro* hybridization with ES cells. *Curr. Biol.* **11,** 1553–1558 (2001).
5. Cowan, C. A., Atienza, J., Melton, D. A. & Eggan, K. Nuclear reprogramming of somatic cells after fusion with human embryonic stem cells. *Science* **309,** 1369–1373 (2005).
6. Jaenisch, R. Human cloning—the science and ethics of nuclear transplantation. *N. Engl. J. Med.* **351,** 2787–2791 (2004).
7. Takahashi, K. & Yamanaka, S. Induction of pluripotent stem cells from mouse embryonic and adult fibroblast cultures by defined factors. *Cell* **126,** 663–676 (2006).
8. Labosky, P. A., Barlow, D. P. & Hogan, B. L. Mouse embryonic germ (EG) cell lines: transmission through the germline and differences in the methylation imprint of insulin-like growth factor 2 receptor (*Igf2r*) gene compared with embryonic stem (ES) cell lines. *Development* **120,** 3197–3204 (1994).
9. Boyer, L. A. *et al.* Core transcriptional regulatory circuitry in human embryonic stem cells. *Cell* **122,** 947–956 (2005).
10. Loh, Y. H. *et al.* The Oct4 and Nanog transcription network regulates pluripotency in mouse embryonic stem cells. *Nature Genet.* **38,** 431–440 (2006).
11. Lee, T. I. *et al.* Control of developmental regulators by Polycomb in human embryonic stem cells. *Cell* **125,** 301–313 (2006).
12. Boyer, L. A. *et al.* Polycomb complexes repress developmental regulators in murine embryonic stem cells. *Nature* **441,** 349–353 (2006).
13. Bernstein, B. E. *et al.* A bivalent chromatin structure marks key developmental genes in embryonic stem cells. *Cell* **125,** 315–326 (2006).
14. Azuara, V. *et al.* Chromatin signatures of pluripotent cell lines. *Nature Cell Biol.* **8,** 532–538 (2006).
15. Jackson-Grusby, L. *et al.* Loss of genomic methylation causes p53-dependent apoptosis and epigenetic deregulation. *Nature Genet.* **27,** 31–39 (2001).
16. Li, E., Bestor, T. H. & Jaenisch, R. Targeted mutation of the DNA methyltransferase gene results in embryonic lethality. *Cell* **69,** 915–926 (1992).
17. Meissner, A. *et al.* Reduced representation bisulfite sequencing for comparative high-resolution DNA methylation analysis. *Nucleic Acids Res.* **33,** 5868–5877 (2005).
18. Ventura, A. *et al.* Cre-lox-regulated conditional RNA interference from transgenes. *Proc. Natl Acad. Sci. USA* **101,** 10380–10385 (2004).
19. Holm, T. M. *et al.* Global loss of imprinting leads to widespread tumorigenesis in adult mice. *Cancer Cell* **8,** 275–285 (2005).
20. Okano, M., Bell, D. W., Haber, D. A. & Li, E. DNA methyltransferases Dnmt3a and Dnmt3b are essential for *de novo* methylation and mammalian development. *Cell* **99,** 247–257 (1999).
21. Stewart, C. L., Stuhlmann, H., Jähner, D. & Jaenisch, R. *De novo* methylation, expression, and infectivity of retroviral genomes introduced into embryonal carcinoma cells. *Proc. Natl Acad. Sci. USA* **79,** 4098–4102 (1982).
22. Jähner, D. *et al. De novo* methylation and expression of retroviral genomes during mouse embryogenesis. *Nature* **298,** 623–628 (1982).
23. Maherali, N. *et al.* Global epigenetic remodeling in directly reprogrammed fibroblasts. *Cell Stem Cells* (in the press)..

24. Mitsui, K. *et al.* The homeoprotein Nanog is required for maintenance of pluripotency in mouse epiblast and ES cells. *Cell* **113,** 631–642 (2003).
25. Chapman, V., Forrester, L., Sanford, J., Hastie, N. & Rossant, J. Cell lineage specific undermethylation of mouse repetitive DNA. *Nature* **307,** 284–286 (1984).
26. Walsh, C. P., Chaillet, J. R. & Bestor, T. H. Transcription of IAP endogenous retroviruses is constrained by cytosine methylation. *Nature Genet.* **20,** 116–117 (1998).
27. Blelloch, R. *et al.* Reprogramming efficiency following somatic cell nuclear transfer is influenced by the differentiation and methylation state of the donor nucleus. *Stem Cells* **24,** 2007–2013 (2006).
28. Lucifero, D., Mertineit, C., Clarke, H. J., Bestor, T. H. & Trasler, J. M. Methylation dynamics of imprinted genes in mouse germ cells. *Genomics* **79,** 530–538 (2002).
29. Hochedlinger, K., Yamada, Y., Beard, C. & Jaenisch, R. Ectopic expression of Oct-4 blocks progenitor-cell differentiation and causes dysplasia in epithelial tissues. *Cell* **121,** 465–477 (2005).
30. Wernig, M. *et al.* Functional integration of embryonic stem cell-derived neurons *in vivo*. *J. Neurosci.* **24,** 5258–5268 (2004).
31. Brambrink, T., Hochedlinger, K., Bell, G. & Jaenisch, R. ES cells derived from cloned and fertilized blastocysts are transcriptionally and functionally indistinguishable. *Proc. Natl Acad. Sci. USA* **103,** 933–938 (2006).
32. Eads, C. A. & Laird, P. W. Combined bisulfite restriction analysis (COBRA). *Methods Mol. Biol.* **200,** 71–85 (2002).
33. Peitz, M., Pfannkuche, K., Rajewsky, K. & Edenhofer, F. Ability of the hydrophobic FGF and basic TAT peptides to promote cellular uptake of recombinant Cre recombinase: a tool for efficient genetic engineering of mammalian genomes. *Proc. Natl Acad. Sci. USA* **99,** 4489–4494 (2002).
34. Eggan, K. *et al.* Hybrid vigor, fetal overgrowth, and viability of mice derived by nuclear cloning and tetraploid embryo complementation. *Proc. Natl Acad. Sci. USA* **98,** 6209–6214 (2001).

Supplementary Information is linked to the online version of the paper at www.nature.com/nature.

Acknowledgements We thank H. Suh, D. Fu and J. Dausman for technical assistance; J. Love for help with the microarray analysis; S. Markoulaki for help with blastocyst injections; F. Edenhofer for a gift of Tat-Cre; and S. Yamanaka for the Nanog-neo construct. We acknowledge L. Zagachin in the MGH Nucleic Acid Quantitation core for assistance with real-time PCR. We also thank C. Lengner, C. Beard and M. Creyghton for constructive criticism. M.W. was supported in part by fellowships from the Human Frontiers Science Organization Program and the Ellison Foundation; B.B. by grants from the Burroughs Wellcome Fund, the Harvard Stem Cell Institute and the NIH; and R.J. by grants from the NIH.

Author Contributions M.W., A.M. and R.J. conceived and designed the experiments and wrote the manuscript; M.W. derived all iPS lines; M.W. and A.M. performed the *in vitro* and *in vivo* characterization of the iPS lines (teratoma, 2N and 4N injections and IHC) and the conditional Dnmt1 experiment; A.M. investigated the promoter and imprinting methylation; M.K. and B.B. performed and analysed the real-time PCRs and ChIP experiments; R.F. and K.H. generated the selectable MEFs and TTFs; R.F. performed western blot and PCR analyses; and T.B. performed the microarray analysis and the proviral integration Southern blots.

Author Information All microarray data from this study are available from Array Express at the EBI (http://www.ebi.ac.uk/arrayexpress) under the accession number E-MEXP-1037. Reprints and permissions information is available at www.nature.com/reprints. The authors declare no competing financial interests. Correspondence and requests for materials should be addressed to R.J. (jaenisch@wi.mit.edu).

METHODS

Cell culture, MEF isolation, gene targeting and viral infections. ES and iPS cells were cultivated on irradiated MEFs in DME containing 15% fetal calf serum, leukaemia inhibiting factor (LIF), penicillin/streptomycin, L-glutamine, and non-essential amino acids. All cells were depleted of feeder cells for two passages on 0.2% gelatin before RNA, DNA or protein isolation. Transgenic MEFs were isolated and selected in 2 μg ml^{-1} puromycin (Sigma) from E13.5 chimaeric embryos after blastocyst injection of Oct4-inducible KH2 ES cells[29] that had been previously targeted with either Oct4-IRES-GFPneo or Nanog-neo constructs (Fig. 1a and ref. 24). Using homologous recombination in ES cells, an IRES-GFPneo fusion cassette was inserted into the *Bcl*I site downstream of *Oct4* exon 5. Correctly targeted ES cell clones were screened by Southern analysis of *Nco*I-digested DNA using a 5′ external probe. The murine cDNAs for *Oct4*, *Sox2*, *Klf4* and *c-myc* were PCR amplified from ES cell cDNA, sequence-verified and cloned into the Moloney-based retroviral vector pLIB (Clontech). 2×10^5 MEFs or TTFs at passage 2–4 were infected overnight with pooled viral supernatant generated by transfection of 4×10^6 HEK293T cells (Fugene, Roche) with 10 μg of viral vectors and the packaging plasmid pCL-Eco in a 10-cm dish[35].

Blastocyst injection. Diploid or tetraploid blastocysts (94–98 h after HCG injection) were placed in a drop of DMEM with 15% FCS under mineral oil. A flat-tip microinjection pipette with an internal diameter of 12–15 mm was used for iPS cell injection (using a Piezo micromanipulator[34]). A controlled number of cells was injected into the blastocyst cavity. After injection, blastocysts were returned to KSOM media and placed at 37 °C until transferred to recipient females.

Recipient females and caesarean sections. Ten to fifteen injected blastocysts were transferred to each uterine horn of 2.5 days post coitum pseudo-pregnant B6D2F1 females. To recover full-term pups, recipient mothers were killed at 19.5 days post coitum. Surviving pups were fostered to lactating BALB/c mothers.

Southern blot, methylation and chromatin analyses. To assess the levels of DNA methylation, genomic DNA was digested with *Hpa*II, and hybridized to pMR150 as a probe for the minor satellite repeats[25], or with an IAP-probe[26]. Bisulphite treatment was performed with the Qiagen EpiTect Kit. For the methylation status of *Oct4* and *Nanog* promoters, bisulphite sequencing analysis was performed as described previously[27]. A total of 10–20 clones of each sample was sequenced in both directions. For imprinted genes, a COBRA assay was performed. PCR primers and conditions were as described previously[28]. PCR products after bisulphite treatment and gel purification were digested with *Bst*UI (CGCG; *H19*, *Peg3* and *Snrpn*) or HpyCH4 IV (ACGT; *Peg1*) and resolved on a 2% agarose gel. Unmethylated CpGs in the recognition sequence will be converted to T and not cut. The status of bivalent domains was determined by chromatin immunoprecipitation followed by quantitative PCR analysis, as described previously[12].

Expression analysis. Fifty nanograms of total RNA isolated using TRIzol reagent (Invitrogen) was reverse-transcribed and quantified using the QuantTtect SYBR green RT–PCR Kit (Qiagen) on a 7000 ABI detection system. Western blot and immunofluorescence analysis was performed as described[29,30]. Primary antibodies included Oct4 (monoclonal mouse, Santa Cruz), Nanog (polyclonal rabbit, Bethyl), actin (monoclonal mouse, Abcam) and SSEA1 (monoclonal mouse, Developmental Studies Hybridoma Bank). Fluorophor-labelled secondary antibodies were purchased from Jackson Immunoresearch. Microarray targets from 2 μg total RNA were synthesized and labelled using the Low RNA Input Linear Amp Kit (Agilent) and hybridized to Agilent whole-mouse genome oligo arrays (G4122F). Arrays were scanned on an Agilent G2565B scanner and signal intensities were calculated in Agilent FE software. Data sets were normalized using an R script (available at http://www.ebi.ac.uk/arrayexpress) and clustered as previously described[31].

Viral integrations. Genomic DNA was digested with *Spe*I (Oct4, c-myc, klf4) or HindIII (Sox2) overnight, followed by electrophoresis and transfer, and the blots were hybridized to the respective radioactively labelled cDNAs of the four transcription factors.

Genotyping. Blastocysts were lysed for 4 h in 10 μl 50 mM Tris, pH 8.8, containing 1 mM EDTA, 0.5% Tween20 and 200 μg ml^{-1} proteinase K. After heat inactivation for 15 min, PCR was performed with the following conditions: 95 °C 30 s (1 cycle); 95 °C 10 s, 60 °C 15 s, 72 °C 15 s (40 cycles); 72 °C 5 min.

Primer sequences for genotyping. GFP-F, TCCATGGCCAACACTAGTCA; GFP-R, TCCCAGAATGTTGCCATCTT; pLIB-FW1, CCCCCTTGAACCTCCTCGTTCGAC; Oct4R, GAGGTTCCCTCTGAGTTGCTTT; MycR, CGAATTTCTTCCAGATATCCTCAC.

Primer sequences for viral-specific qRT–PCR. rtKlf4_virusF1, TCTCTAGGCGCCGGAATTC; rtKlf4_virusR1, CCATGTCAGACTCGCCAGGT; rtMyc_virusF1, CTTCTCTAGGCGCCGGAATT; rtMyc_virusR1, TGGTGAAGTTCACGTTGAGGG; rtOct4_virusF1, TACACCCTAAGCCTCCGCCT; rtOct4_virusR1, ATTCCGGCGCCTAGAGAAG; rtSox2_virusF1, TACACCCTAAGCCTCCGCCT; rtSox2_virusR1, ATTCCGGCGCCTAGAGAAG.

***Dnmt1* hairpin target sequence DZ.** GGAAAGAGATGGCTTAACA.

35. Naviaux, R. K., Costanzi, E., Haas, M. & Verma, I. M. The pCL vector system: rapid production of helper-free, high-titer, recombinant retroviruses. *J. Virol.* **70**, 5701–5705 (1996).